Electronic structure approach for complex silicas

Alexander A. Demkov
Department of Physics and Astronomy, Arizona State University, Tempe, Arizona 85287

José Ortega*
Cavendish Laboratory, University of Cambridge, Cambridge CB3 0HE, United Kingdom

Otto F. Sankey and Matthew P. Grumbach
Department of Physics and Astronomy, Arizona State University, Tempe, Arizona 85287
(Received 14 March 1995)

We develop a theoretical electronic structure based approach suitable for the study of complex silicas, and apply it to three different silica polymorphs. The method is first principles but simplified to cope with large systems. Charge transfer between ions is included in a self-consistent fashion. The method is found to be adequate to describe the relative energetics and the electronic structure of silica and is used to construct a simplified model energy for the structural transition of high cristobalite. In addition we have studied the moderately complex silica, melanophlogite. Melanophlogite, although a clathrate structure belonging to the group of silica polymorphs known as clathrasils, is found to be only 10 kJ/mol above α-quartz, in accord with the recent thermochemical study of the stability of zeolites.

I. INTRODUCTION

Silica or silicon dioxide is one of the most abundant and important materials on earth, and as such is one of the most thoroughly studied. Silica is known to exist in numerous polymorphs, the variety of which is attributed to the large number of possible topologies obtained by linking the relatively rigid corner-sharing SiO_4 tetrahedra. The unit cells for complex silicas can in some cases involve hundreds or even thousands of atoms, as is the case for complex zeolites.

Almost all the available atomic theories have been applied to silica: empirical potentials, semiempirical tight-binding, *ab initio* solid state methods, and quantum chemistry methods. Empirical potentials have been used with a certain success to describe the phase diagram and phase transitions,[1–3] but the intricate balance between the ionic and covalent components of bonding is apparently beyond the appealing simplicity of these methods.[4] Semiempirical tight-binding techniques have been employed to study the electronic structure of bulk crystalline polymorphs, defects, and SiO_2 glasses.[5–7] The limited transferability of the tight-binding parameters, however, leads to well-known difficulties in describing the geometrical arrangement of atoms. The necessity of reliable and fast first-principles methods for complex systems can hardly be overemphasized.

Despite the industrial importance of silica and the vast body of experimental work, the number of first-principles studies of silica remains relatively small, both from quantum chemistry and solid state physics perspectives. Only recently have *ab initio* density functional theory (DFT) or Hartree-Fock methods been successfully applied to study solid state properties of a number of silica polymorphs.[8–15] Despite the obvious successes of existing first-principles methods, one must not overlook their limitations. The structural "softness" of the Si-O-Si bridges makes the energetics delicate, and requires a high degree of convergence for the theory to be quantitative. In the popular plane-wave pseudopotential (DFT) method, for example, this requirement is confronted with two major difficulties: The unit cell must not be too large (the computation scales as the cube of the number of electrons, N), and the presence of first-row elements (e.g., oxygen) generally requires the use of an enormous number of plane waves. A comprehensive account of applications of quantum chemistry methods to silica may be found in Ref. 16.

There is an immediate need for a fast *ab initio* method allowing a unified approach to the electronic structure, total energy, and dynamical properties of systems such as silica polymorphs. The purpose of this paper is to present such a method and to demonstrate its usefulness with some applications to the silica minerals. In particular, we investigate the structural transition in high cristobalite. We use the results of the first-principles calculations to derive a simple phenomenological model describing this transition. The model enables us to obtain an analytical expression for the Si-O bond length as a function of the bond angle. Finally, we perform an *ab initio* calculation of the zeolite melanophlogite.

The paper is organized as follows: In Sec. II we discuss the proposed theoretical model; in Sec. III we apply this method to determine the energetics and the electronic structure of α-quartz, β-cristobalite, and the zeolite melanophlogite.

0163-1829/95/52(3)/1618(13)/$06.00

II. THEORY

A. Background

The plane-wave total energy method based on the local density approximation (LDA) to density functional theory (DFT) and the pseudopotential technique has proved to be quite successful when applied to a variety of solids. The computational efficiency of this method has been significantly improved in the last decade. Although new developments have made possible the study of systems containing a number of atoms of roughly an order of magnitude larger than before, the method is still computationally very demanding both in CPU time and memory requirements.[17–20]

At the same time, the alternative local-orbital approach to DFT has seen a quieter revolution. In 1985, Harris[21] introduced an approximate energy expression, known since then as the Harris functional (or the Harris-Foulkes functional[22]). This energy expression is obtained by expanding the Kohn-Sham energy about a reference electron density, and the reference potential constructed from that electron density, with an error which is second order with respect to the deviation of the reference electron density from the self-consistent one (ρ_{SC}). Foulkes and Haydock[22] have remarked that the electron density and the one-electron potential may, in principle, be treated as independent variables, resulting in a more general functional. In a different line of development, an approximate linear combination of atomic orbitals (LCAO) Hamiltonian has been obtained by means of a second-quantization formalism.[23] In this approach, the many-body terms are included without resorting to the usual LDA approximation.[24] This procedure avoids the problems associated with the LDA exchange and correlation effects in the description of hydrogen bonds[25] or other weakly bonded systems.[26]

Two important features of the Harris functional E_H, as compared with the non-self-consistent Kohn-Sham functional E_{KS}, are that (i) E_H is far easier to evaluate and (ii) E_H gives a better estimate of the ground state energy E_0 when the electron density ρ is not ρ_{SC}. Probably, the main advantage of the Harris functional is the possibility of choosing an appropriate form for the *input* (reference) charge density which is a sum of densities localized at various sites, together with the use of localized orbitals to solve the one-particle Schrödinger equation. The electron-electron Coulomb integrals are at most three center, which is a great simplification. Input densities consisting of the sum of the free atomic densities have been used in the calculation of several properties of some dimers[21,22] and solids,[27–29] with remarkable results. However, the accuracy is significantly improved if, instead of free atomic densities, use is made of "contracted" atomic densities.[29–32]

Another important step towards a fast and accurate total energy method consists of choosing an efficient basis set for the determination of the occupied eigenvalues and eigenvectors of the one-particle Schrödinger equation. Sankey and Niklewski[30] have introduced the "fireball" basis, in which the orbitals are obtained by solving the atomic problem with the boundary condition that the "atomic" orbitals vanish outside and at a predetermined radius R_c. An important advantage of this basis set is that the Hamiltonian (and overlap) matrix elements have a short range. This method was extended by Drabold *et al.* to systems with disparate types of atoms.[33] Ordejón *et al.* have implemented an order-N technique using this method so that the computation time scales linearly with the size of the system for large systems.[34] Recently Lin and Harris[35] have proposed the use of a LCAO orbital basis of Λ functions, which are linearly related to Slater-type orbitals (STO's). In their approach, the exponents associated with the orbitals are optimized, resulting in a more flexible scheme at the price of higher computational effort. The use of Slater-type orbitals requires that the contribution of many distant neighbors needs to be calculated. However, if one is interested in describing weak interactions (such as hydrogen bonds[25] or the interaction between noble-gas atoms and a solid surface[26]) the STO's are probably the most convenient basis set.

The Sankey-Niklewski-Drabold (SND) method has proved to be a very efficient and successful tool for a great variety of problems.[36] However, the representation of the input electron density $\rho(\vec{r})$ by a sum of *neutral* atomiclike charge densities limits the applicability of the SND method when there is an important difference in the electronegativity of the atoms that constitute the system under study. The aim of the theoretical work presented here is to generalize the SND method to deal with systems which present a significant transfer of charge between atoms (like the silicas), while keeping all the features that makes it so efficient, and capable of handling complex systems. The major features that the theory maintains are (i) a short-range nonorthogonal local orbital basis; (ii) all the analysis is done in real space (the use of reciprocal lattice vectors is forbidden, except in a simple Ewald summation); (iii) integrals involving four centers are not required in the Harris scheme, so that all the two- and three-center integrals are easily tabulated beforehand and placed on interpolation grids no larger than two dimensional; (iv) molecular dynamics simulations are performed by looking up the necessary integrals from the interpolation grids.

B. Method

The Harris expression for the total energy of a system of electrons and ions for an input charge density ρ_0 is

$$E_{\rm tot}[\rho] = \left[\sum_i \epsilon_i\right] + [E_{ii} - E_{ee}(\rho_0)] + \left[E_{\rm xc}(\rho_0) - \int \rho_0(\vec{r})\mu_{\rm xc}(\rho_0(\vec{r}))d^3r\right], \quad (1)$$

where the ϵ_i's are the occupied eigenvalues of the single-particle Hamiltonian,

$$\left(-\frac{\hbar^2}{2m}\nabla^2 + V[\rho_0]\right)\psi_i = \epsilon_i\psi_i, \quad (2)$$

with

$$V[\rho_0] = \sum_{\vec{R}_\alpha} V_{\rm ion}^{\alpha}(\vec{r} - \vec{R}_\alpha) + e^2 \int \frac{\rho_0(\vec{r'})d^3r'}{|\vec{r} - \vec{r}'|} + \mu_{\rm xc}(\rho_0(\vec{r})). \tag{3}$$

$V_{\rm ion}^{\alpha}$ is the ionic pseudopotential of the atom at $\vec{R}_\alpha$, $E_{\rm xc}(\rho_0)$ is the LDA exchange-correlation energy, $\mu_{\rm xc}(\rho_0(\vec{r}))$ is the exchange-correlation potential, E_{ii} is the ion-ion repulsion, and

$$E_{ee} = \frac{e^2}{2} \int\int \frac{\rho_0(\vec{r})\rho_0(\vec{r'})}{|\vec{r} - \vec{r}'|} d^3r d^3r' \tag{4}$$

is the electron-electron repulsion.

In our approach we represent the *input* electron density ρ_0 as a sum of charged atoms of different *s-p* hybridizations as

$$\rho_0(\vec{r}) = \sum_i n_i |\phi_i(\vec{r} - \vec{R}_i)|^2. \tag{5}$$

Here the n_i are real positive numbers that define the occupation of the "atomic" orbital ϕ_i on the atom at position $\vec{R}_i$. The orbitals $\phi_i(\vec{r} - \vec{R}_i)$ are the slightly excited pseudoatomic orbitals ("fireballs") of Sankey and Niklewski[30] that are used as basis functions to solve the one-particle equation (2). The input density $\rho_0(\vec{r})$ is a sum of confined spherical atomiclike densities, each of them with a number of electrons determined by its occupation number n_i. Allowing n_i to vary implies that the distribution of charge around each atom (taking into account the nuclear charge) is in general *non-neutral*, and we must deal with long-range interactions. The value of n_i will depend on the chemical environment of the orbital $\phi_i(\vec{r} - \vec{R}_i)$, through the density associated with the single-particle orbital ψ_i, and its practical determination will be discussed below.

The occupation numbers n_i can be written down as the sum of a neutral, n_i^0, and a non-neutral contribution, δn_i:

$$n_i = n_i^0 + \delta n_i. \tag{6}$$

Here n_i^0 is an appropriate reference occupation number that gives a "neutral-atom" charge density (e.g., $n_s^0 = n_p^0 = 2$ for Si), and δn_i describes the charge transfer between the atoms of the system. The input electron density [Eq. (5)] induces a one-electron potential [Eq. (3)] which has both long-range (due to the δn_i) and short-range contributions to the single-particle Hamiltonian matrix elements $h_{\alpha\beta}$:

$$h_{\alpha\beta} = \left\langle \phi_\alpha(\vec{r} - \vec{R}_\alpha) \left| \left(-\frac{\hbar^2}{2m}\nabla^2 + V[\rho_0] \right) \right| \phi_\beta(\vec{r} - \vec{R}_\beta) \right\rangle = h_{\alpha\beta}^{\rm SR} + h_{\alpha\beta}^{\rm LR}. \tag{7}$$

The matrix element $h_{\alpha\beta}^{\rm SR}$ contains the contributions due to the kinetic energy, ionic pseudopotential, and "neutral-atom" Hartree and exchange-correlation potentials. We refer the reader to Ref. 30 for a detailed discussion of the short-range term $h_{\alpha\beta}^{\rm SR}$. The exchange-correlation matrix elements are readily obtained due to an elegant linearization described in Ref. 30. In the following subsection we discuss an approximate and efficient (fast) way of calculating the long-range Hartree contribution $h_{\alpha\beta}^{\rm LR}$ to the single-particle Hamiltonian matrix elements $h_{\alpha\beta}$. Our aim is to keep the method fast and efficient, with, of course, paying as small a price as possible concerning accuracy.

C. Long-range contribution to the single-particle Hamiltonian

The long-range part of the single-particle Hamiltonian matrix elements, $h_{\alpha\beta}^{\rm LR}$, can be written as

$$h_{\alpha\beta}^{\rm LR} = e^2 \sum_i \delta n_i g_{\alpha\beta}^i, \tag{8}$$

where

$$g_{\alpha\beta}^i = \left\langle \phi_\alpha(\vec{r} - \vec{R}_\alpha) \left| \int \frac{|\phi_i(\vec{r'} - \vec{R}_i)|^2 d^3r'}{|\vec{r} - \vec{r}'|} \right| \phi_\beta(\vec{r} - \vec{R}_\beta) \right\rangle. \tag{9}$$

The functions g are three-center integrals, but due to the short-range nature of the fireball orbitals, we notice that $g_{\alpha\beta}^i = 0$ if $|\vec{R}_\alpha - \vec{R}_\beta| > [R_c(\alpha) + R_c(\beta)]$ [$R_c(\gamma)$ is the cutoff radius for the orbital ϕ_γ described in the Introduction].

In the more interesting situation in which $|\vec{R}_\alpha - \vec{R}_\beta| < [R_c(\alpha) + R_c(\beta)]$, we have two cases: (i) the near field and (ii) far field regimes.

(i) The near field regime is defined to be where both orbitals in the matrix element overlap the density $|\phi_i(\vec{r'} - \vec{R}_i)|^2$, i.e., where $|\vec{R}_\alpha - \vec{R}_i| < [R_c(\alpha) + R_c(i)]$ *and* $|\vec{R}_\beta - \vec{R}_i| < [R_c(\beta) + R_c(i)]$. In this case the integral $g_{\alpha\beta}^i$ is calculated numerically. The results for all possible geometries are stored on a two-dimensional (2D) grid of distances and interpolated when needed. This procedure is identical to that described in Ref. 30 for the neutral-atom matrix elements, and the details may be found in that paper.

(ii) The far field regime is where either one or both of the orbitals in the matrix element do not overlap the charge density, i.e., $|\vec{R}_\alpha - \vec{R}_i| > [R_c(\alpha) + R_c(i)]$ *or* $|\vec{R}_\beta - \vec{R}_i| > [R_c(\beta) + R_c(i)]$ (or both).

These are the true long-range contributions to the matrix element $h_{\alpha\beta}$ and the geometry is shown schematically in Fig. 1. An infinite number of atomic centers i contributes, in principle, to the matrix element $h_{\alpha\beta}$. However, the physics in Eq. (9) is simply electrostatics, and we make use of far field electrostatic approximations. To further simplify our task we shall consider only the the most important matrix elements and set the rest to zero as discussed below. Since the wave function densities $|\phi_i(\vec{r} - \vec{R}_i)|^2$ are spherically symmetric and normalized (for p states, we take a suitable spherical average), we have that in the far field regime

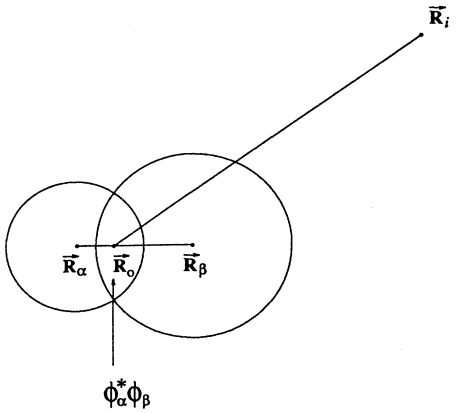

FIG. 1. Geometry of the Coulomb integrals for near and far fields (see text).

$$g^i_{\alpha\beta} = \int \frac{\phi^*_\alpha(\vec{r}-\vec{R}_\alpha)\phi_\beta(\vec{r}-\vec{R}_\beta)}{|\vec{r}-\vec{R}_i|} d^3r. \quad (10)$$

The product $\phi^*_\alpha\phi_\beta$ may have a dipole moment, and so we expand $\frac{1}{|\vec{r}-\vec{R}_i|}$ in Legendre polynomials to yield

$$g^i_{\alpha\beta} = \frac{S_{\alpha\beta}}{|\vec{R}_i-\vec{R}_o|} + \frac{1}{|\vec{R}_i-\vec{R}_o|^3}(\vec{R}_i-\vec{R}_o).\vec{p}_{\alpha\beta}(\vec{R}_o) + \cdots \quad (11)$$

(see Fig. 1), where

$$S_{\alpha\beta} = \int \phi^*_\alpha(\vec{r}-\vec{R}_\alpha)\phi_\beta(\vec{r}-\vec{R}_\beta)d^3r \quad (12)$$

is the overlap (charge) and $p_{\alpha\beta}$ is the dipole moment,

$$\vec{p}_{\alpha\beta}(\vec{R}_o) = \int \phi^*_\alpha(\vec{r}-\vec{R}_\alpha)\phi_\beta(\vec{r}-\vec{R}_\beta)(\vec{r}-\vec{R}_o)d^3r. \quad (13)$$

We are free to choose our "origin" $\vec{R}_o$ so that the second (dipolar) term in Eq. (10) vanishes. Doing this we obtain that $g^i_{\alpha\beta}$ is approximately

$$g^i_{\alpha\beta} = \frac{S_{\alpha\beta}}{|\vec{R}_i-\vec{R}_m-[\vec{p}_{\alpha\beta}(\vec{R}_m)/S_{\alpha\beta}]|}. \quad (14)$$

Here, $\vec{R}_m = (\vec{R}_\alpha+\vec{R}_\beta)/2$.

Within the same order of approximation, this can be simplified further by defining effective charges q_α and q_β on each of the orbitals and writing Eq. (14) in the more convenient form

$$g^i_{\alpha\beta} = \frac{q_\alpha}{|\vec{R}_i-\vec{R}_\alpha|} + \frac{q_\beta}{|\vec{R}_i-\vec{R}_\beta|}, \quad (15)$$

with effective charges $q_\alpha = \frac{1}{2}S_{\alpha\beta} + p_{\alpha\beta}(\vec{R}_m)/d_{\rm BC}$ and $q_\beta = \frac{1}{2}S_{\alpha\beta} - p_{\alpha\beta}(\vec{R}_m)/d_{\rm BC}$, where $d_{\rm BC}$ is the "bond charge" distance $d_{\rm BC} = |\vec{R}_\alpha - \vec{R}_\beta|$ and $p_{\alpha\beta}(\vec{R}_m)$ is the dipole along $\vec{d}_{\rm BC}$. Terms for which either $S_{\alpha\beta}$ or the dipole moment in the bond charge direction vanish are set to zero. Equation (15) is now a sum of two-center terms and the infinite sum of contributions to the matrix element $h_{\alpha\beta}$ from all atoms i is now summable exactly using standard Ewald summation techniques.

Physically, the approximations of Eq. (9) to yield Eq. (15) have included monopole and dipole far field effects. These are used to calculate the contribution to $h^{\rm LR}_{\alpha\beta}$ of all the densities $|\phi_i(\vec{r}-\vec{R}_i)|^2$ whose charge distribution does not overlap with the bond charge $\phi^*_\alpha(\vec{r}-\vec{R}_\alpha)\phi_\beta(\vec{r}-\vec{R}_\beta)$ [case (ii) above]. In the near field [case (i)], the integral is computed exactly and includes all multipoles. However, at the boundary between case (i) and case (ii), there will be a small discontinuity in the value of $g^i_{\alpha\beta}$ due to the far field approximations. We remove this discontinuity by "smoothing" the boundary between the two regimes of approximation:

$$g^i_{\alpha\beta} = f(r)g^i_{\alpha\beta}[\text{Eq. (9)}] + [1-f(r)]g^i_{\alpha\beta}[\text{Eq. (15)}], \quad (16)$$

where r is the distance from the center of the density to the center of the bond charge. The smoothing function $f(r)$ we choose is unity for distance up to second nearest neighbors, and drops smoothly to zero at about third neighbors.

D. Determination of the occupation numbers n_i's

The total energy [Eq. (1)] is a function of the occupation numbers n_i,

$$E_{\rm tot}[\rho_0] \equiv E_H(n_i), \quad (17)$$

once we have restricted the input density to be of the form given by Eq. (5). The problem is thus reduced to finding out which are the n_i's that give the best estimate for the ground state energy $E_0 = E_H[\rho_{\rm SC}]$.

The Harris energy expression is stationary at $\rho_{\rm SC}$,[21,22] but it is neither a maximum nor a minimum; i.e., in general the stationary point at $\rho_{\rm SC}$ is a saddle point.[37,38] Several authors have pointed out that the Harris energy functional displays a maximum at its stationary point ($\rho = \rho_{\rm SC}$) for a wide class of densities ρ.[29,28,39] The input density of Eq. (5) seems to belong to that class of densities, and use could be made of the *maximum* property of the Harris energy expression to determine the optimum set of n_i's.[35] Recently, Methfessel[40] has shown that when the density and the potential are considered as independent variables[22] the energy functional is maximal respective to the potential and minimal respective to the density. This means that in our case we could use two sets of independent n_i's (one to characterize the potential and the other for the density) and optimize them accordingly.

However, one must be especially careful once the long-range Coulomb interaction is explicitly included in the theory since it can, if not treated carefully, give nonphysical results. To illustrate this point we consider a simple dimer with a transfer of charge between the two atoms, and compare the electrostatic contributions (ES's) to the total energy in the limit of large separation. In the Har-

ris theory, one obtains the "band structure" contribution $E_{\rm BS}^{\rm ES}$ from summing energy eigenvalues:

$$E_{\rm BS}^{\rm ES} = 2E_{ee}(n^{\rm in}, n^{\rm out}) + E_{ei}(n^{\rm out}), \tag{18}$$

where $n^{\rm in}$ is the input electron density and $n^{\rm out}$ is the output electron density obtained from the single-particle wave function. In addition to the band structure energy is the ion-ion and electron-electron "double-counting" correction:

$$E_{\rm DC}^{\rm ES} = E_{ii} - E_{ee}(n^{\rm in}, n^{\rm in}). \tag{19}$$

If we now add Eqs. (18) and (19) for the dimer case in which one atom on input has excess charge δq^0 and the other $-\delta q^0$, while on output has corresponding charges δq and $-\delta q$, we obtain, for large d,

$$E_{\rm total}^{\rm ES}(d) = \frac{e^2}{d}\delta q^0(-\delta q + (\delta q^0 - \delta q)) + U_0, \tag{20}$$

where U_0 does not depend on d, the distance between the two atoms of the dimer. As one can see, for the neutral input density ($\delta q^0 = 0$) the $1/d$ contribution to $E_{\rm total}^{\rm ES}$ vanishes, while for a self-consistent density ($\delta q^0 = \delta q$) the long-range effects result in the proper $-e^2(\delta q)^2/d$ attraction. However, for a non-self-consistent density ($\delta q^0 \neq \delta q$), Eq. (20) can result in either an attractive interaction or a repulsive interaction. If the input and output charges are significantly different, we obtain the nonphysical result that the two oppositely charged atoms repel. The mathematical condition which leads to this nonphysical result from Eq. (20) is $\delta q < \frac{\delta q^0}{2}$.

We have found this effect in fact to occur for the case of a Si-O dimer under certain conditions. Here the Si atom donates some of its electrons to the oxygen atom. If we incorporate poor "guesses" for the input charge transfer, we find that the two atoms of the Si-O dimer repel for large distances. This is shown in Fig. 2. In Fig. 2 we show the total energy of a Si-O dimer as a function of the interatomic separation obtained by a self-consistent calculation (labeled SCF on the graph) and by three non-self-consistent calculations: one for two neutral atoms and two for the atoms with the fixed charge transfer (the amount of charge transferred is indicated in the graph). As one can see, both the self-consistent and Harris (neutral) calculations result in physical long-range limits (the atoms attract). However, when the transfer of charge is allowed in the non-self-consistent calculation, a guess which is close to the self-consistent solution ($\delta q = 0.25$) deviates only slightly from the correct answer, while a "bad" guess ($\delta q = 0.5$) results in the aforesaid unphysical repulsion at separations larger than 2.25 Å.

This example demonstrates the need for some level of self-consistency. However, the representation of the input electron density in the form given by Eq. (5) prevents us from achieving self-consistency in the standard way, where $\rho^{\rm in}(\vec{r}) = \rho^{\rm out}(\vec{r})$ at each point r. One simplified way to obtain an approximate solution was proposed by Averill and Painter.[31] In their method, the density is written as a superposition of the fit-basis functions with unknown coefficients, and the output charge density of

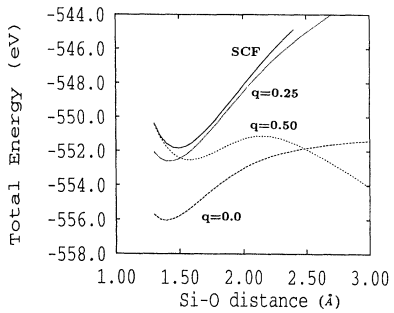

FIG. 2. The total energy of a Si-O dimer as a function of the interatomic separation obtained by a self-consistent calculation (labeled SCF) and by the three non-self-consistent calculations, one for the two neutral atoms and two for the atoms with the fixed charge transfer (the amount of charge transferred is indicated in the graph). Note that for large distances the interaction is repulsive for the curve labeled $q = 0.5$.

the previous iteration cycle is used to determine these coefficients subject to the constraint of conservation of the total number of electrons, by a conventional least-squares fit.

In the present work, we have followed an approach that is similar in concept to Ref. 31 but is simplified and less computationally intense. We define output occupation numbers $n_i^{\rm out}$ as

$$n_i^{\rm out} = 2\sum_\alpha |\langle\psi_\alpha|\varphi_i\rangle|^2, \tag{21}$$

where ψ_α are the occupied eigenvalues of Eq. (2) and φ_i are the atomiclike orthogonal orbitals of Löwdin,[41]

$$\varphi_i = \sum_j (\mathbf{S}^{-\frac{1}{2}})_{ij}\phi_j. \tag{22}$$

We determine the occupation factors $n_i^{\rm out}$ from the "self-consistency" condition $n_i^{\rm out} = n_i$ for all i, where n_i is the input occupation numbers from Eq. 5. Equation (21) may be viewed as a way of projecting the *output* electron density obtained from Eq. (2) into a density of the form given by Eq. (5). This scheme is similar to the one of Ref. 42, where Mulliken charges were used in a self-consistent charge Hartree-Fock-Slater model.

We next apply this theoretical method to the study of several silica polymorphs. We use a minimal basis set consisting of sp^3 orbitals on the silicon and oxygen atoms. The cutoff radii R_c have been chosen to be $R_c(\mathrm{O}) = 3.6$ and $R_c(\mathrm{Si}) = 5.0$ (atomic units). Improvements in this basis set, such as an optimized choice of the R_c's or the inclusion of more orbitals (e.g., d orbitals) per atom, are certainly possible, and will be analyzed in the future.

III. RESULTS

The most common crystalline phases of SiO_2 are α- and β-quartz, α- and β-cristobalite, stishovite, β-trydimite, and coesite. These different polymorphs are

TABLE I. Experimental crystal parameters for the pure SiO_2 polymorphs α-quartz, β-cristobalite, and for the clathrasil melanophlogite.

Polymorph	Space group Table No.[a]	Lattice constants (Å)	Atoms/cell	Si-O-Si angles	Si-O bond length Å
α-quartz[b]	$P3_221$	$a = 4.916$	9	143.7°	1.614-1.605
	No. 154	c=5.4054			Avg=1.610
	Trigonal				
β-cristobalite[c]	$I\bar{4}2d$	$a = 5.042$	12	146°	1.62
	No. 122	$c = 7.131$			
	Hexagonal				
melanophlogite[d]	$Pm\bar{3}n$	$a = 13.436$	138	148.3-180.0°	1.569-1.595
	No. 223			Avg=168.8°	Avg=1.576
	Cubic				

[a]Space group number in *International Tables of X-ray Crystallography* (The Kynoch Press, Birmingham, England, 1965).
[b]B.G. Hyde and S. Anderson, *Inorganic Crystal Structures* (Wiley, New York, 1989).
[c]A.F. Wright and A.J. Leadbetter, Philos. Mag. **31**, 1391 (1975).
[d]H. Gies, Z. Kristallogr. **164**, 247 (1983).

stable in different parts of the pressure-temperature phase diagram. In addition to the pure polymorphs, there exists yet another family of silica polymorphs which are impure. These are the clathrate compounds known as clathrasils and include silica-sodalite, dodecasil $1H$, decadodecasil $3R$, melanophlogite, nonasil, and dodecasil $3C$. In all these silica polymorphs, except high-pressure stishovite, oxygen atoms are twofold coordinated, forming a continuous three-dimensional framework of nearly regular SiO_4 tetrahedra linked by sharing corners. The tetrahedra are fairly rigid within themselves; it is the variety of ways they may be linked by corner sharing that is responsible for the great multitude of silica polymorphs. Silica also exists in amorphous or glassy phases, in addition to the above-mentioned crystalline phases.

Correctly predicting the relative stability of the complex set of structures for silica is a considerable challenge for any theoretical method. Most of these polymorphs have energies very close to each other, so that subtle effects due to the bond angles must be correctly included in the theory to properly describe trends. One expects that a careful Hartree-Fock or LDA Kohn-Sham calculation would obtain realistic results, but these calculations are quite demanding.

We have tested our method by calculating the equation of state for the three silica polymorphs: α-quartz, β-cristobalite, and melanophlogite. The experimental structures of these polymorphs are given in Table I, and the experimental fractional internal parameters are given in Table II. The energy vs volume curves we obtain are shown in Fig. 3. In this figure we have fixed the fractional internal coordinates to those of experiment, and have used experimental values for the c/a ratios for those structures with two lattice constants. When the full relaxation is performed for α-quartz we obtain $V = 34.842$ Å^3/molecule, $B = 34.74$ GPa, and $B' = 6.61$, for the equilibrium volume, the bulk modulus, and its derivative, respectively. We have used a Murnaghan

TABLE II. Experimental coordinates for the pure SiO_2 polymorphs α-quartz, β-cristobalite, and for the clathrasil melanophlogite.

Polymorph	Fractional coordinates	x	y	z
α-quartz[a]	$O_1(6c)$ xyz, etc.	0.4135[b]	0.2669	0.1191
	$Si_1(3a)$ $x00$, etc.	0.4697		
β-cristobalite[c]	O_1 $(8d)$ $x\frac{1}{4}\frac{1}{8}$, etc.	-0.09		
	Si_1 $(4a)$ 000, etc.			
Melanophlogite[c]	$O_1(48l)$ xyz, etc.	0.0963	0.2465	0.1360
	$O_2(24k)$ $0yz$, etc.		0.4056	0.1813
	$O_3(12f)$ $x00$, etc.	0.3423		
	$O_4(8e)\frac{1}{4}\frac{1}{4}\frac{1}{4}$, etc.			
	$Si_1(24k)$ $0yz$, etc.		0.3098	0.1142
	$Si_2(16i)$ xxx, etc.	0.1826		
	$Si_3(6c)\frac{1}{4}0\frac{1}{2}$, etc.			

[a]B.G. Hyde and S. Anderson, *Inorganic Crystal Structures* (Wiley, New York, 1989).
[b]α-quartz is shifted by $[0,0,-\frac{1}{3}]$ from the *International Tables of X-ray Crysallograplhy* (The Kynoch Press, Birmingham, England, 1965) so that the unit cells of α- and β-quartz correspond.
[c]A.F. Wright and A.J. Leadbetter, Philos. Mag. **31**, 1391 (1975).
[d]H. Gies, Z. Kristallogr. **164**, 247 (1983).

equation of state to determine the bulk modulus (B), and have found B to be quite sensitive. The energy vs volume curves have very appreciable nonparabolic contributions, and points needed to be chosen very close to the minimum. The results for β-cristobalite shown in Fig. 3 are for the ideal (but incorrect) $C9$ structure which assumes linear Si-O-Si bonds. The correct β-cristobalite E vs volume curves are much "softer" due to the changes in the Si-O-Si angle, as will be discussed separately below. The most important result of Fig. 3, however, is that a correct ground state structure (α-quartz) is found. The energetics of β-cristobalite and melanophlogite will be discussed below, but it appears that the melanophlogite energy minimum is quite reasonable when compared to similar experimentally measured silicas, while the energy of β-cristobalite appears somewhat high.

The electronic band structures for the three polymorphs of this study are shown in Fig. 4. The zero of energy is defined to be the top of the valence band in all cases. All structures show bands which are quite similar in major features. There is an oxygen s-state-derived set of bands in the range -17 to -22 eV depending on the structure. The next highest set of bands is the oxygen-silicon bonding orbital bands centered at around -7 to -8 eV. The highest set of occupied bands is the nonbonding p_π states on the oxygen. These states form the top of the valence band. The band gaps are quite large; we find $\sim$16 eV for α-quartz. Experimentally the band gap of α-quartz is 9.2 eV,[43–45] although the size of the gap cannot be said to be well established due to the formation of excitons and defects. The use of the LDA is well known to predict gaps below those of experiment, while the use of a minimal basis set of local orbitals (the main effect here) is known to increase[46] the band gap above experiment.

The density of states for α-quartz has been measured by ultraviolet and x-ray photoemission.[47,48] It is found that the lowest peak exists at $\sim$21 eV below the top of the valence band, while our bands indicate a peak at about $\sim$20 eV. The next set of peaks corresponding to the O-Si bonding states are at ~ -10 and -7.5 eV, while our bands indicate peaks at ~ -9 and -6 eV. The final p_π band experimentally peaks at ~ -2.5 eV and is about 5 eV wide, while our band is centered at ~ -2 eV and is $\sim$ 4 eV wide. Thus our results for the overall electronic structure are in a good agreement with the experimental data, and we feel confident enough to apply this method to study in detail the structural properties of high cristobalite.

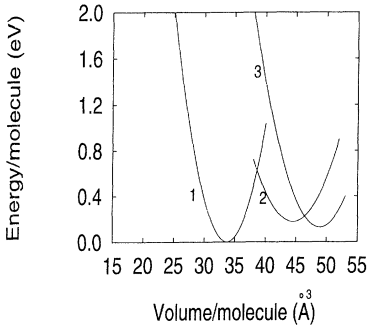

FIG. 3. Total energy vs volume for three silica polymorphs (1) α-quartz, (2) β-cristobalite, (3) melanophlogite, obtained using the current *ab initio* method.

A. Structural properties of high cristobalite

High cristobalite (or β-cristobalite) is one of the most intriguing of all the silica polymorphs. Being metastable under ambient conditions (cristobalite is stable just below the SiO_2 melting point) this polymorph occurs naturally, and was named after the San Cristobal Desert in Mexico where it can be found. The reason for cristobalite being easily quenched to room temperature lies in the reconstructive nature of the α-quartz to cristobalite transformation (the very strong Si-O bonds have to be broken). The structure of β-cristobalite was proposed by Wyckoff[49] over 50 years ago to be the linear Si-O-Si $C9$ structure, which is now believed to be incorrect. The details of the correct structure remain controversial, although there appears to be a general consensus on the most important parameters.

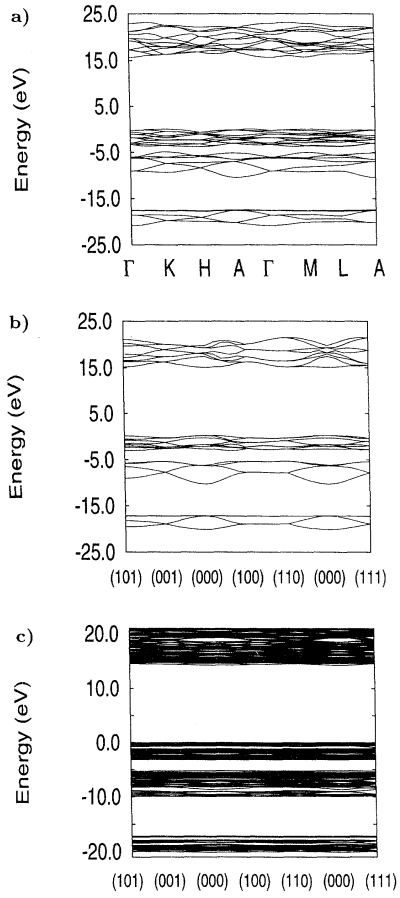

FIG. 4. Band structures of silica polymorphs (a) α-quartz, (b) β-cristobalite, (c) melanophlogite, obtained using the current *ab initio* method.

In the idealized $C9$ structure proposed by Wyckoff the Si atoms take positions on a diamond structure, and oxygen atoms take positions at the bond centers midway between two Si atoms. The Si-O-Si bond is therefore linear, and the resulting structure is cubic and belongs to space group $Fd\bar{3}m$ with Si in the $8a$ positions and O in the $16c$ positions. The lattice constant of the material leads to the conclusion that the Si-O bond length is 1.54 Å, which is very short compared to that in other SiO_2 polymorphs. What is perhaps more important, however, is that the Si-O-Si bond angle is 180°, and not the characteristic 145°–150°. Nieuwenkamp[50] proposed that the material is disordered and only the average symmetry is $Fd\bar{3}m$, and there exists a local configuration of bent Si-O-Si bonds. Leadbetter[51] and Wright and Leadbetter[52] in more recent experiments proposed that the correct structure of high cristobalite is a distortion from $C9$ with the lower local symmetry of $I\bar{4}2d$, which gives an Si-O-Si angle of 147° and a bond length of 1.61 Å. A continuous transformation from the $C9$ structure to the $I\bar{4}2d$ structure was shown by O'Keeffe and Hyde[53] to be accomplished by rotating corner-sharing rigid SiO_4 tetrahedra by an angle ϕ about a $\bar{4}$ axis in opposite directions. During the rotation, the Si-O-Si angle is reduced from the linear value (180°), to smaller angles down even to the tetrahedral angle of 109.47°. At the tetrahedral angle, the structure has collapsed into a defective chalcopyrite structure, which can be thought of as a zinc-blende structure with every other cation missing. The average $Fd\bar{3}m$ structure can be obtained by random static domains of $I\bar{4}2d$. However, this view is controversial, and an alternative view is that there exist domain walls of α-cristobalite between domains of β-cristobalite[54] or that the β-cristobalite structure is dynamically distorted with an average structure of $Fd\bar{3}m$.[55]

There have been few theoretical investigations of this polymorph. Vashishta *et al.*[2] used a classical two- and three-body potential to find the volume-dependence of several (fixed) SiO_2 crystal structures, including "ideal" β-cristobalite ($C9$) and a bent bond structure. They find that the $C9$ structure is the lowest-energy β-cristobalite structure and the α-cristobalite structure to be the ground state silica polymorph. Zhang and Ong[3] have recently theoretically investigated the possibility of the pressure-induced amorphization in this structure by means of the constant-pressure molecular dynamics and find amorphization to a six-coordinated structure at 11–15 GPa. Keskar and Chelikowsky[8] have used a classical three-body potential to investigate the pressure dependence of the six internal parameters for the $Fd\bar{3}m$ structure as defined by Wyckoff. Welberry *et al.*[56] have performed Monte Carlo simulations using a Born–von Karman harmonic force model. When the model is modified to constrain the Si-O-Si angle to 147°, the predicted diffraction pattern is in good agreement with the experimental one. Recently there have been two *ab initio* theoretical studies of β-cristobalite. Silvi *et al.*[15] have performed periodic Hartree-Fock calculations on the related α-cristobalite, relaxing the tilt angle. They find that the $C9$ structure (which occurs at a tilt angle 0°) to be dynamically unstable. Liu *et al.*[14] have examined the $C9$, $I\bar{4}2d$, and $P2_13$ structures using a Kohn-Sham plane-wave technique. They find that of these three the $I\bar{4}2d$ structure is energetically favored.

The continuous set of possible β-cristobalite structures may be described most simply in terms of just two parameters: the Si-O bond length d and the corner-sharing tetrahedron rotation angle ϕ. In this model, the SiO_4 tetrahedra are assumed to remain regular. Given a fixed bond length d, the rotational angle ϕ=0° corresponds to the linear $C9$ structure, while ϕ=45° corresponds to the tetrahedral defective chalcopyrite structure. A general value of ϕ results in the $I\bar{4}2d$ structure. The relation between ϕ and the Si-O-Si bond angle Θ is

$$\cos\Theta = \frac{1 - 4\cos^2\phi}{3}. \tag{23}$$

The structure refinement of Wright and Leadbetter corresponds to the $I\bar{4}2d$ structure with rotational angle ϕ=19.8°.

We find this picture attractive since it has only two parameters, and allows us to explore the entire "structural space" of the $I\bar{4}2d$ structure. In Fig. 5 we show the energy per molecule of β-cristobalite as a function of the rotational angle ϕ for different Si-O bond lengths d. From this figure, we see that shorter bond lengths favor the linear $C9$ structure, while the longer bond lengths favor the distorted structure with nonlinear Si-O-Si bonds. In no case is the defective chalcopyrite structure ($\phi = 45°$) the structure lowest in energy. The global minimum occurs for a value of d = 1.56 Å, and at the distortion angle of $\phi = 20.5°$. Our bond length is systematically underestimated by about 0.05 Å in all structures.

We can rationalize this behavior as arising from competing interactions within the crystal. The "orbital" Si(sp^3)-O(p_σ) interactions favor a 90° Si-O-Si configuration,[57] while the Si-Si nonbonding overlap repulsion together with the repulsive Coulomb contributions between adjacent Si atoms try to keep the Si atoms as far away from each other as possible, thus favoring the collinear 180° configuration. When the bond length is short, the distance between adjacent Si atoms is reduced and the system seeks the $C9$ linear structure since it allows the two silicon atoms to be farther away. When

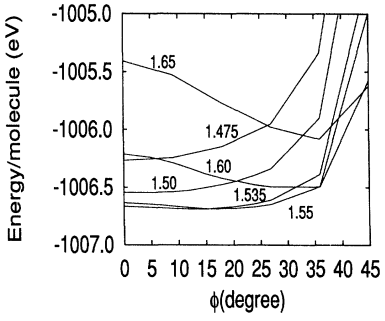

FIG. 5. Energy of β-cristobalite as a function of tetrahedron rotational angle ϕ for the different Si-O bond lengths. The angle ϕ determines the Si-O-Si bond angle through Eq. (23).

the bond length is increased, the system seeks the lowest energy by compromising the orbital Si(sp^3)-O(p_σ) interaction and the Si-Si repulsion.

It is illuminating to cast the theory of the transition between the idealized $Fd\bar{3}m$ Wyckoff $C9$ structure and the experimental $I\bar{4}2d$ structures along the lines of a Landau theory of phase transitions.[58] We write an approximate energy function involving the two independent variables in this model which are the Si-O bond length d, and the rotation angle ϕ between rigid tetrahedra, as

$$E(d,\phi) = E_0 + \frac{1}{2}k(d-d_b)^2 + \frac{1}{2}\kappa_2(d)\phi^2 + \frac{1}{4!}\kappa_4(d)\phi^4. \tag{24}$$

Here the Si-O distance d plays the role of a generalized temperature, and the rotational angle ϕ that of the order parameter. The first term E_0 is a constant which sets the zero of energy. The second term is an Si-O bond-stretching term of "spring constant" k and equilibrium distance d_b. We include both harmonic and anharmonic bond-bending terms, with d-dependent spring constants $\kappa_2(d)$ and $\kappa_4(d)$. Symmetry does not allow a cubic κ_3 term. Notice that our expansion is performed around $\phi = 0$, the linear Si-O-Si $C9$ system.

As will be seen below, the bond-bending coefficient $\kappa_2(d)$ depends on the bond length d, and in fact vanishes at some critical bond length d^* (which plays a role of the "critical temperature"). We expand κ_2 in a Taylor series to first order in the bond length as

$$\kappa_2(d) = \kappa_0\left(1 - \frac{d}{d^*}\right), \tag{25}$$

where d^* is the transition bond length in which the bond-bending spring at $\phi = 0$ vanishes. The "spring" κ_4 is not expected to change sign, so we replace the coefficient $\kappa_4(d)$ by $\kappa_4(d^*) = \kappa_4$ for simplicity, leading to our simplified energy function

$$E(d,\phi) = E_0 + \frac{1}{2}k(d-d_b)^2 + \frac{1}{2}\kappa_0\left(1-\frac{d}{d^*}\right)\phi^2 + \frac{1}{4!}\kappa_4\phi^4. \tag{26}$$

Our model energy contains the parameters E_0, k, d_b, κ_0, d^*, and κ_4 which we obtain from a fit of our first-principles calculations. The constants E_0, d_b, and k are readily obtained from calculations of the linear $C9$ structure. In Fig. 6 we show the energy as a function of the Si-O distance (ϕ=0°), which evidently shows a parabolic behavior which determines the first two terms of Eq. (26). To obtain two of the remaining three parameters, we calculate the energy as a function of the bond length for a small angle ϕ. Assuming that the quartic term can be neglected, we can then use Eq. (26) to determine $\kappa_2(d)$, which is shown in Fig. 7. The bond distance d at which $\kappa_2(d)$ crosses the axis determines d^*, and the slope determines κ_0.

The "critical" parameter d^* is perhaps the most important in the model, since it quantifies the transition from the $C9$ to $I\bar{4}2d$ structure. For $d < d^*$, the energy curves vs ϕ are concave upward with increasing ϕ (a restoring force), while for $d > d^*$, they are concave downward, producing an instability which breaks the symmetry.

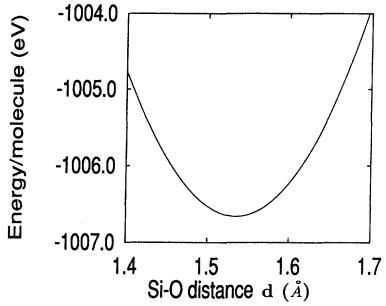

FIG. 6. Energy of the $C9$ structure ($\phi = 0$) as a function of the Si-O bond length, obtained from our *ab initio* method. A parabolic fit determines the model parameters E_0, k, and d_b.

The final parameter κ_4, the anharmonicity parameter, is obtained from fitting any single point of the curves in Fig. 5 close to the transition. The term $\kappa_4\phi^4$ in the energy expression Eq. (26) makes large ϕ angles (small θ angles) very unfavorable. The values we obtain from the fit are given in Table III. The energies predicted by the model and the parameters of Table III are shown in Fig. 8. This figure should be compared to the results of the *ab initio* calculations in Fig. 5. The zero-pressure minimum energy structure is found by imposing $\partial E/\partial d = \partial E/\partial\phi = 0$. The vanishing of $\partial E/\partial d$ leads to

$$d_{\min} = d_b + (\kappa_0/k)\phi^2_{\min}, \tag{27}$$

which illustrates that for parameters which yield a minimum energy structure with a large tilt angle $\phi_{\min}$ (i.e., smaller Si-O-Si bond angle), the bond length increases, and vice versa. The vanishing of $\partial E/\partial\phi$ yields a cubic equation with roots $\phi_{\min} = 0$ or $\phi_{\min} = \pm\sqrt{\frac{-3!\kappa_0(1-d/d^*)}{\kappa_4}}$. The first solution is the $C9$ structure, while the second set of solutions yield the lower-symmetry $I\bar{4}2d$ structure. Either solution ($C9$ or $I\bar{4}2d$) is possible within this model depending on the choice of parameters. In terms of model parameters only, the solutions are given by $d_{\min} = d^*\frac{(d_b-\eta)}{(d^*-\eta)}$, where $\eta =$

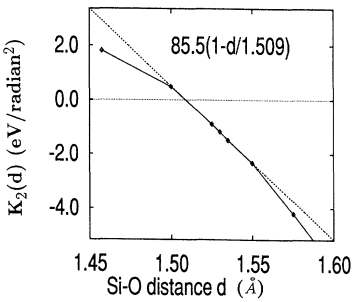

FIG. 7. Model parameter $\kappa_2(d)$ as a function of the Si-O bond length d. Diamonds indicate values computed from *ab initio* energies. The bond distance at which $\kappa_2 = 0$ determines d^*, and the slope determines κ_0.

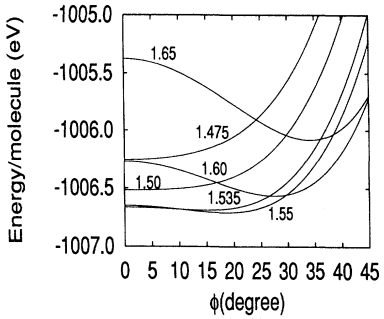

FIG. 8. Energy of β-cristobalite as a function of rotation angle ϕ for different Si-O bond lengths, obtained from the model energy function. The parameters for the model were obtained using the current *ab initio* method (see Table III).

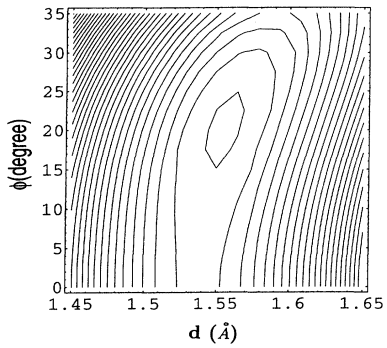

FIG. 9. Contour plot of energy of β-cristobalite as a function of rotation angle ϕ and Si-O bond length d, obtained from the model energy function with parameters determined by the current *ab initio* local orbital method.

$\frac{3!\kappa_0^2}{2d^*k\kappa_4}$, and $\phi_{\min} = \sqrt{\frac{3!(d_{\min}-d^*)\kappa_0}{d^*\kappa_4}}$. Using the parameters given in Table III, we obtain the $I\bar{4}2d$ structure with $d_{\min}$=1.56 Å and $\phi_{\min}$=0.358 rad = 20.525° (which corresponds to the Si-O-Si angle θ = 146.73°). Experimental values of Wright and Leadbetter[52] are $d \approx$1.6 Å and $\phi \approx$19.8 (θ = 147.88°). We view this agreement with experiment as being exceptionally good, and suggest that our simplified first-principles technique is capable of distinguishing the subtle energetics of complex silicas.

The simple model gives in analytical terms an important fact of silica studies: many low-energy structures can be found with large θ values (small ϕ values), but structures with small θ values (low ϕ values) are rare or of high energy.[59] The mathematical statement of these facts in this model is that κ_2 is soft (actually crossing zero), making small ϕ structures cost little in energy, while κ_4 is more or less constant, making large ϕ structures energy expensive because of the ϕ^4 barrier.

Using Eq. (26), we have constructed a contour plot of the energy as a function of the bond length and the tilt angle. This is shown in Fig. 9 and shows the characteristic "thumbprint" plot, which is very similar to one obtained for silicate fragments by Gibbs,[60] who used quantum chemistry methods.

As a check on our conclusion and on the theoretical method itself, we have performed similar calculations using the much more rigorous Kohn-Sham (LDA) plane-wave technique. The solutions are obtained iteratively using a preconditioned conjugate gradient method.[61,62] The pseudopotential for oxygen was generated using the method of Troullier and Martins,[63] while the silicon pseudopotential was generated with Vanderbilt's method.[64] Plane waves up to 50 Ry are included, and three special points in the irreducible wedge are used to sample the Brillouin zone. The model parameters derived from these calculations are given in Table III. The minimum energy predicted by the model occurs at $d_{\min}$ =1.67 Å and $\phi_{\min}$ =13.3°. A contour plot of the energy as a function of bond length and tilt angle is shown in Fig. 10.

A useful heuristic "rule of thumb" can be formulated: In order for the contour plot to be bent to the right (indicating that the $I\bar{4}2d$ structure is the ground state), d^* (the critical length) should be less than d_b the bond length of minimum energy for the $C9$ structure. This rule may be used to sort out semiempirical models with the correct physics built in from those constructed by simple fitting. For example results obtained using the potential of van Beest *et al.*,[65] shown in Fig. 11, show no clear change in the second derivative with respect to ϕ for small ϕ, and thus κ_2 has no clear change in sign (see Fig. 11). Such a potential would not predict the correct "thumbprint" as in Fig. 9 or 10.

The correlation between the tetrahedral d(Si-O) bond lengths and the $\angle$ Si-O-Si bond angles in a wide range of silicas has been studied by several authors.[53,60,66] It has been shown by means of regression analysis that d(Si-O) depends almost linearly on $-\sec(\angle\text{Si-O-Si})$. If we assume a general applicability of the Eq. (26) to *all* silicas, we can express the $\angle$ Si-O-Si angle in terms of d(Si-O) using the parameters of Table III. The result is shown in Fig. 12, where we have shifted the curve down by 0.05 Å to compensate for our systematic underestimate of the bond length. Also included in Fig. 12 are the regression analysis of Hill and Gibbs[66] and the experimental data from Ref. 67 for comparison. The two curves are in qualitative but not quantitative agreement. This is not unexpected since we are using the parameters from cristobalite and

TABLE III. Parameters of the energy model [Eq. (26)] computed using the current local orbital method and a SC plane-wave method.

Method	E_0	k (eV/Å^2)	d_b (Å)	κ_0 (eV/rad^2)	d^* (Å)	κ_4 (eV/rad^4)
Current method	-1006.66	206.1508	1.538	85.5	1.509	123.54
SC plane-wave method	-975.778	197.357	1.663	41.02	1.531	206.546

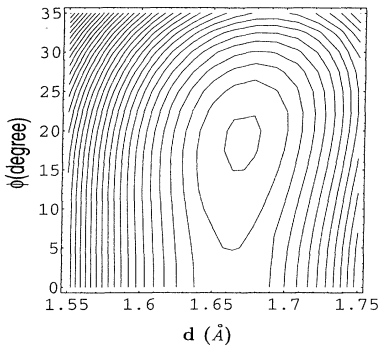

FIG. 10. Contour plot of energy of β-cristobalite as a function of rotation angle ϕ and Si-O bond length d, obtained from the model energy function with parameters determined by the self-consistent plane-wave pseudopotential method.

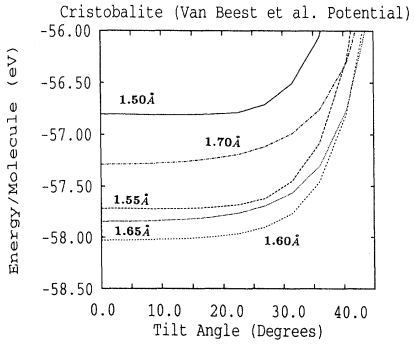

FIG. 11. Same as Fig. 8, the parameters for this plot were obtained using the method of Ref. 65.

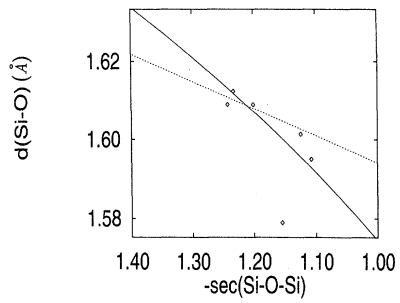

FIG. 12. Dependence of d(Si-O) on $-\sec(\angle$Si-O-Si) obtained using Eq. (26) (solid line). Also for comparison, results of regression analysis of Ref. 66 (dashed line) and experimental data of Ref. 67 are shown.

ignore all topological variation of geometry in the silica family. There is of course enormous scatter in the data, indicating that no simple formula can be expected to give quantitative agreement. But it is gratifying that such a simple result as that given in Eq. (26) fairly accurately describes this important correlation.

In conclusion, we have applied our technique to the study of β-cristobalite, and find general agreement with the experiment and previous *ab initio* calculations. We proposed a simple phenomenological model describing the structural properties of this phase, with the six parameters of the model being readily obtained from any first-principles (or empirical) calculations. In the future it may also be possible to turn the problem around and extract the model parameters from experimental data, which would provide a convenient means to gauge the accuracy of *ab initio* calculations.

B. Melanophlogite

Melanophlogite is a rare mineral, and belongs to the group of silica polymorphs known as clathrasils.[68] It is a clathrate compound whose structure consists of polyhedral cages of SiO_2, which encapsulate impurity atoms. The structure contains up to 8% of C, H, O, N, and S in the form of guest molecules entrapped within the cages of the host framework. The SiO_2 framework is constructed of corner-sharing SiO_4 tetrahedra. The Si 3D four-connected network itself makes the polyhedral cages of which there are two types: dodecahedra (a polyhedron with 12 pentagonal faces) and tetrakaidecahedra (a polyhedron with 14 faces, 2 of which are hexagonal, while the rest are pentagonal). This structure has 46 SiO_2 molecules (138 atoms) per unit cell containing 2 dodecahedra and 6 tetrakaidecahedra. Stereographic representations of the structure can be found in Refs. 69–71. The framework is isostructural with that of cubic type-II gas hydrates containing impure H_2O.[72] This connection between clathrate silicas and water has been examined by Kamb.[73] Elemental silicon also takes this form in the presence of a high impurity concentration of alkali-metal atoms, as in the silicon clathrates M_xSi_{46} and M_xSi_{136} (M stands for the alkali-metal atom).[74,75] The pure Si form has a band gap predicted to be 0.7 eV higher than diamond Si, and when doped with some metals has a Jahn-Teller distortion and flat band with a high density of states at the Fermi level.[70,76] The structure has channels going in (100) directions, with the apertures formed by hexagonal rings.

Naturally occurring melanophlogite is tetragonal, while the synthetic one is cubic with the space group $Pm\bar{3}n$ and a=13.436 Å at 200 °C.[71] Upon heating, natural melanophlogite transforms to a cubic phase at about 60 °C, although this temperature varies from locality to locality and from sample to sample. For example Gies[71] reports that samples from Mt. Hamilton (California) transform at 65°, while no transformation is seen up to 150 °C for samples from Sicily. Presumably this is due to variations in the guest species and concentration. Here we will examine the cubic modification in the absence of

impurities.

The coordinates of the structure are given in Table II. As can be seen, there are three different types of sites occupied by silicon[71] and four different types of sites occupied by oxygen. Some of the Si-O-Si bond angles are 180° ($\phi = 0$), which according to the Eq. (26) should give rise to shorter bond lengths. This is indeed the case. The average bond length in this structure is 1.576 Å, which is significantly shorter than typical silica bond lengths of 1.60–1.61 Å. The average angle is 168.8°, which is 20° wider than typical silicas.

We have performed the *ab initio* calculation of melanophlogite. We have not incorporated any guest molecules into the structure, but consider the "idealized" melanophlogite. It is not clear *a priori* whether the structure is significantly higher in energy than other naturally occurring pure silicas, and is found in nature only because the guest impurities have drastically altered the energy of the structure, or that the ideal structure is actually competitive in energy with other structures, and the guest atoms only slightly modify the energy and are acting as a template for the melanophlogite cage crystals to grow around them.

Total energy calculations can give some information concerning this point. We have calculated the total energy and electronic states for this structure. Due to the large number of internal parameters, we have not done a full optimization of the structure, but used the experimental fractional coordinates (given in Table II) and dilated or contracted the lattice. The band structure is shown in Fig. 4. We find melanophlogite to be a direct (Γ-to-Γ) gap material with a large band gap of 14.3 eV or almost 2.0 eV lower than that found for α-quartz. The valence band has the structure very similar to that of α-quartz, with the oxygen s band being shifted slightly up in energy. The results of this calculation for the energy as a function of volume for melanophlogite are shown in Fig. 3. We find the minimum energy lattice constant to be 13.11 Å which gives a volume per molecule of 49.04 Å^3. The volume is thus expanded from α-quartz by over 40%. Our values can be compared to the experimental values of 13.43 Å for the lattice constant and 52.66 Å^3 for the volume, which show we have errors of 2.8% and 6.9%, respectively. The bond lengths range from 1.53 to 1.56 Å compared to the experimental range of 1.57–1.60 Å. Again our results give bond lengths which are systematically about 3% too short. An estimated value of the bulk modulus is 126.1 GPa, but the internal coordinates were not optimized at each volume. The most significant result is that we find melanophlogite to be only 0.1 eV/molecule (10 kJ/mol) above α-quartz. This result is in a good agreement with the recent thermochemical study of Petrovic *et al.*[59] who find that structures of large volume are typically 0.10–14 kJ/mol above α-quartz. These authors find almost no correlation between the energy of zeolite structures and the average bond angle, but suggest that it is rather the distribution of these angles that is important. In particular, the presence of small angles (under 140°) is the major destabilizing factor; e.g., faujasite is the least stable zeolite structure (0.14 eV/molecule above α-quartz) in their study, and it has the largest fraction of small angles. Melanophlogite does not have bond angles below 145°, which may explain its relative stability with respect to quartz.

IV. CONCLUSIONS

In conclusion, in this paper we have presented a fast *ab initio* total energy method, and applied it to the study of several properties of the silica polymorphs. The key features of the theory presented here are the use of the energy expression due to Harris,[21] together with the representation of the input electron density in the form given by Eq. (5) and the use of an appropriate short-range basis set ("fireball" local orbitals[30]) to solve the one-particle Schrödinger equation (2). The resulting calculational scheme is orders of magnitude faster than standard *ab initio* methods.

In Sec. III we have presented the results for α-quartz, β-cristobalite, and melanophlogite. A simple model for the structural transition of high cristobalite is suggested. This model can be used to interpret the correlation between the Si-O bond lengths and bond angles in a variety of silica polymorphs. We have performed an *ab initio* calculation of the zeolite melanophlogite, and find it to be 0.1 eV/molecule above α-quartz. This is in qualitative agreement with recent experimental trends which indicate very small energies of zeolites above those of quartz.

ACKNOWLEDGMENTS

We thank the NSF High Pressure Material Synthesis MRG (Grant No. DMR-9121570) and the Office of Naval Research (Grant No. ONR 00014-90-J-1304). J.O. would like to thank European Community Human Capital and Mobility Fund for financial support. It is our pleasure to thank Professor Michael O'Keeffe and Professor Paul McMillan for many insightful discussions that we had in the course of this work. We thank Professor Richard Martin for his interest and helpful comments. We also wish to thank David Teter for his comments on the manuscript. J.O. wishes to thank Professor Volker Heine for stimulating conversations, encouragement, and for a pleasant stay at Cambridge, and also thanks Dr. Rubén Pérez for stimulating conversations.

* Present address: Departamento de Física de la Materia Condensada, Universidad Autonoma de Madrid, E-28049 Madrid, Spain.

[1] S. Tsuneyuki, M. Tsukada, H. Aoki, and Y. Matsui, Phys. Rev. Lett. **61**, 869 (1988).

[2] P. Vashishta, R. K. Kalia, and J. Rino, Phys. Rev. B **41**, 12 197 (1990).

[3] X. Zhang and C. Ong, Phys. Rev. B **48**, 6865 (1993).

[4] J. Chelikowsky, H. E. King, Jr., N. Troullier, J. L. Martins, and J. Glinnemann, Phys. Rev. Lett. **65**, 3309 (1990).
[5] L. Stixrude and M. Bukowinski, Phys. Rev. B **44**, 2523 (1991).
[6] E. P. O'Reilly and J. Robertson, Phys. Rev. B **27**, 3780 (1983).
[7] Y. Xu and W. Ching, Phys. Rev. B **44**, 11 048 (1991).
[8] N. Keskar and J. Chelikowsky, Phys. Rev. B **46**, 1 (1992).
[9] N. Binggeli and J. Chelikowsky, Nature **353**, 344 (1991).
[10] J. Chelikowsky, N. Troullier, J. Martins, and J. H. E. King, Phys. Rev. B **44**, 489 (1991).
[11] D. Allan and M. Teter, Phys. Rev. Lett. **59**, 1136 (1987).
[12] D. Allan and M. Teter, J. Am. Ceram. Soc. **73**, 3247 (1990).
[13] X. Gonze, D. Allan, and M. Teter, Phys. Rev. Lett. **68**, 3603 (1992).
[14] F. Liu, S. Garfolini, R. King-Smith, and D. Vanderbilt, Phys. Rev. Lett. **70**, 2750 (1994).
[15] B. Silvi, M. Allavena, Y. Hannachi, and P. D'Arco, J. Am. Ceram. Soc. **75**, 1239 (1992).
[16] B. Silvi, J. Mol. Struct. **226**, 129 (1991).
[17] P. Hohenberg and W. Kohn, Phys. Rev. **136**, B864 (1964).
[18] W. Kohn and L. J. Sham, Phys. Rev. **140**, A1133 (1965).
[19] J. Ihm, A. Zunger, and M. L. Cohen, J. Phys. C **12**, 4409 (1979).
[20] R. Car and M. Parrinello, Phys. Rev. Lett. **55**, 2471 (1985).
[21] J. Harris, Phys. Rev. B **31**, 1770 (1985).
[22] W. Foulkes and R. Haydock, Phys. Rev. B **39**, 12 520 (1989).
[23] F. J. García-Vidal, A. Martín-Rodero, F. Flores, J. Ortega, and R. Pérez, Phys. Rev. B **44**, 11 412 (1991).
[24] F. J. García-Vidal, J. Merino, R. Pérez, R. Rincón, J. Ortega, and F. Flores, Phys. Rev. B **50**, 10 537 (1994).
[25] J. Ortega, J. P. Lewis, and O. F. Sankey, Phys. Rev. B **50**, 10 516 (1994).
[26] R. Pérez, F. J. García, P. L. Andrés, and F. Flores, Surf. Sci. **307-309**, 704 (1994).
[27] H. M. Polatoglou and M. Methfessel, Phys. Rev. B **37**, 10 403 (1988).
[28] A. Read and R. Needs, J. Phys. Condens. Matter **1**, 7565 (1989).
[29] M. Finnis, J. Phys. Condens. Matter **2**, 331 (1990).
[30] O. F. Sankey and D. J. Niklewski, Phys. Rev. B **40**, 3979 (1989).
[31] F. Averill and G. Painter, Phys. Rev. B **41**, 10 344 (1990).
[32] H. M. Polatoglou and M. Methfessel, Phys. Rev. B **41**, 5898 (1990).
[33] D. A. Drabold *et al.* (unpublished).
[34] P. Ordejón, D. A. Drabold, M. P. Grumbach, and R. M. Martin, Phys. Rev. B **48**, 14 646 (1993).
[35] Z. Lin and J. Harris, J. Phys. Condens. Matter **5**, 1055 (1993).
[36] G. B. Adams and O. F. Sankey, Phys. Rev. Lett. **67**, 867 (1991); G. B. Adams, O. F. Sankey, J. B. Page, and M. O'Keeffe, Science **256**, 1792 (1992); A. A. Demkov and O. F. Sankey, Phys. Rev. B **48**, 2207 (1993).
[37] B. Farid, V. Heine, G. E. Engel, and I. Robertson, Phys. Rev. B **48**, 11 602 (1993).
[38] I. Robertson and B. Farid, Phys. Rev. Lett. **66**, 3265 (1991).
[39] E. Zaremba, J. Phys. Condens. Matter **2**, 2479 (1990).
[40] M. Methfessel (unpublished).
[41] P. Löwdin, J. Chem. Phys. **18**, 365 (1950).
[42] A. Rosén, D. E. Ellis, H. Adachi, and F. W. Averill, J. Chem. Phys. **65**, 3629 (1976).
[43] Y. Xu and W. Y. Ching, Phys. Rev. B **44**, 11 048 (1991).
[44] B. Fisher, R. Pollak, T. DiStefano, and W. Grobman, Phys. Rev. B **15**, 3193 (1977).
[45] G. Klein and H. Chun, Phys. Status Solidi B **49**, 167 (1972).
[46] R. W. Jansen and O. F. Sankey, Phys. Rev. B **36**, 6520 (1987).
[47] T. H. DiStefano and D. E. Eastman, Phys. Rev. Lett. **27**, 560 (1971).
[48] H. Ibach and J. E. Rowe, Phys. Rev. B **10**, 710 (1974).
[49] R. Wyckoff, Am. J. Sci **9**, 448 (1925).
[50] W. Nieuwenkamp, Z. Kristallogr. **96**, 454 (1937).
[51] A. Leadbetter, T. Smith, and A. Wright, Nature Phys. Sci. **244**, 125 (1973).
[52] A. Wright and A. Leadbetter, Philos. Mag. **31**, 1391 (1975).
[53] M. O'Keeffe and B. Hyde, Acta. Crystallogr. Sect. B **32**, 2923 (1977).
[54] D. M. Hatch and S. Ghose, Phys. Chem. Min. **17**, 554 (1991).
[55] I. P. Swainson and M. T. Dove, Phys. Rev. Lett **71**, 3610 (1993).
[56] T. R. Welberry, G. L. Hua, and R. L. Withers, J. Appl. Cryst. **22**, 87 (1989).
[57] W. Harrison, *Electronic Structure and the Properties of Solids* (W. H. Freeman and Company, San Francisco, 1980), p. 258.
[58] L. D. Landau, Zh. Eksp. Teor. Fiz. **7**, 627 (1937).
[59] I. Petrovic, A. Navrotsky, M. Davis, and S. I. Zones, Chem. Mater. **5**, 1805 (1993).
[60] G. V. Gibbs, Am. Mineral. **67**, 421 (1982).
[61] I. Štich, R. Car, M. Parrinello, and S. Baroni, Phys. Rev. B **39**, 4997 (1989).
[62] M. P. Teter, M. C. Payne, and D. C. Allan, Phys. Rev. B **40**, 12 255 (1989).
[63] M. Troullier and J. Martins, Phys. Rev. B **43**, 1993 (1991).
[64] D. Vanderbilt, Phys. Rev. B **32**, 8412 (1985).
[65] B. W. H van Beest, G. J. Kramer, and R. A. van Santen, Phys. Rev. Lett. **64**, 1995 (1990).
[66] R. I. Hill and G. V. Gibbs, Acta Crystallogr. Sect. B **35**, 25 (1979).
[67] J. V. Smith and C. S. Blakckwell, Nature **303**, 223 (1983).
[68] F. Liebau, Zeolites **3**, 191 (1983).
[69] W. Meier and D. Olson, *Atlas of Zeolite Structure Types*, 3rd ed. (Butterworth-Heineman, London, 1992).
[70] G. B. Adams, M. O'Keeffe, A. A. Demkov, O. F. Sankey, and Y. Huang, Phys. Rev. B **49**, 8048 (1994).
[71] H. Gies, Z. Kristallogr. **164**, 247 (1983).
[72] W. F. Claussen, J. Chem. Phys. **19**, 259 (1951).
[73] B. Kamb, Science **148**, 232 (1965).
[74] C. Cros, M. Pouchard, and P. Hagenmuller, C. R. Acad. Sci. (Paris) **260**, 4764 (1965).
[75] J. Kasper, P. Hagenmuller, M. Pouchard, and C. Cros, Science **150**, 1713 (1965).
[76] A. A. Demkov, O. F. Sankey, K. E. Schmidt, G. B. Adams, and M. O'Keeffe, Phys. Rev. B **50**, 17 001 (1994).